PHYSICAL REVIEW C VOLUME 41, NUMBER 3 MARCH 1990

Dispersion relation for effective interactions

B. V. Carlson and T. Frederico
Centro Técnico Aeroespacial, Instituto de Estudos Avançados, 1231 São José dos Campos, São Paulo, Brazil

M. S. Hussein
Instituto de Física, Universidade de São Paulo, Caixa Postal 20516 São Paulo, São Paulo, Brazil

H. Esbensen and S. Landowne
Physics Division, Argonne National Laboratory, Argonne, Illinois 60439

(Received 25 August 1989)

It is argued that the real and imaginary parts of the effective potential operator for scattering problems obey a dispersion relation also when the Hamiltonian is not Hermitian. Model calculations are used to demonstrate that the equivalent local potential approximately satisfies the dispersion relation when absorption is present. It is also shown that the equivalent local potential is insensitive to the bare potential used in the entrance channel.

I. INTRODUCTION

The recent discoveries of energy-dependent effective interactions in analyses of nuclear scattering data at energies near the Coulomb barrier have generated considerable interest. An important unifying concept in this development is the dispersion relation between the real and imaginary parts of the effective interaction.[1,2] Denoting the formal operator for the effective potential in the entrance channel by $\hat{V}_{\rm pol}$, the dispersion relation is written as

$$\mathrm{Re}\hat{V}_{\rm pol}(E) = -\frac{\mathrm{P}}{\pi}\int_{E_t}^{\infty} dE' \frac{\mathrm{Im}\hat{V}_{\rm pol}(E')}{E-E'} , \qquad (1)$$

where E is the available energy, E_t is the threshold energy for nonelastic processes, and P indicates that the principal part of the integral is to be taken.

For the case where the elastic channel 1 couples via the interaction operator $\hat{V}$ to an inelastic channel 2, one obtains[3]

$$\hat{V}_{\rm pol}(E) = \hat{V}_{12}\frac{1}{E-\hat{H}_2+i\epsilon}\hat{V}_{21} , \qquad (2)$$

where $\hat{H}_2$ is the Hamiltonian in channel 2 and the limit $\epsilon \to 0$ is to be taken. Equation (1) is often recovered by invoking the relation

$$\frac{1}{E-H+i\epsilon} = \mathrm{P}\frac{1}{E-H} - i\pi\delta(E-H) \qquad (3)$$

in the limit $\epsilon \to 0$.

The elegance of the dispersion relation in Eq. (1) is notable. On the other hand, it says nothing specific about the physical mechanisms which cause the energy dependence of the effective interaction. Also the formal operator in Eq. (2) is conceptually quite removed from the local optical potential parametrizations which are used to extract the energy-dependent effects empirically. For a deeper insight one requires model calculations that explicitly account for couplings to nonelastic channels.

Such models for nuclear collisions are invariably based on Hamiltonians that are not Hermitian. This is not simply because of practical difficulties in dealing with many open reaction channels. Typically, a large part of the reaction cross section is due to the complete fusion process which is not modeled by coupling to an open scattering channel, as is assumed in Eq. (2). Discussions of the dispersion relation for the effective interaction usually do not consider non-Hermitian Hamiltonians. For instance, Eq. (3) does not separate the real and imaginary parts of the propagator in this case.

For these reasons, it is interesting to reexamine the effective interaction generated by the type of models which are actually used in practice. In this work we first give a heuristic argument for the dispersion relation in Eq. (1) when the Hamiltonian is not Hermitian. We then present numerical results from model calculations which illustrate how the equivalent local potential follows the behavior expected from the formal potential operator. This provides an intermediate supporting link between the abstract operator formalism and the energy-dependent optical potential parametrizations which are used empirically.

II. DISPERSION RELATION

The dispersion relation for the effective interaction can be derived by applying the following mathematical relation:

$$\mathrm{P}\int_{-\infty}^{+\infty} dE' \frac{f(E')}{E'-E} = i\pi f(E) . \qquad (4)$$

This result holds for any function f of a complex variable E which is analytic on the real axis and in the upper-half E plane and vanishes as $E \to \infty$. Expressing Eq. (4) in real and imaginary parts leads immediately to the relations

©1990 The American Physical Society

$$\mathrm{Re} f(E)=\frac{\mathrm{P}}{\pi}\int_{-\infty}^{+\infty} dE' \frac{\mathrm{Im} f(E')}{E'-E} , \tag{5}$$

$$\mathrm{Im} f(E)=-\frac{\mathrm{P}}{\pi}\int_{-\infty}^{+\infty} dE' \frac{\mathrm{Re} f(E')}{E'-E} , \tag{6}$$

which are referred to mathematically as Hilbert transforms and physically as the Kramers-Krönig relations (see, e.g, Ref. 4).

Consider the effective interaction of Eq. (2) when the Hamiltonian is Hermitian. We distinguish this case by writing

$$\hat{H}_2=\hat{R}=\hat{H}_2^- . \tag{7}$$

Introducing the complete set of eigenstates of $\hat{R}$,

$$\hat{R}|\Phi_r\rangle=E_r|\Phi_r\rangle , \tag{8}$$

into Eq. (2), we can write

$$\hat{V}_{\mathrm{pol}}(E)=\sum_r \frac{\hat{V}_{12}|\Phi_r\rangle\langle\Phi_r|\hat{V}_{21}}{E-E_r+i\epsilon} , \tag{9}$$

under the assumption that the eigenstates of $\hat{R}$ are scattering states.[3] Since $\hat{R}$ is Hermitian, its eigenvalues E_r are real. Consequently, the E dependence of Eq. (9) satisfies the requirements for Eq. (4), the poles being below the real axis. Thus the real and imaginary parts of $\hat{V}_{\mathrm{pol}}$ satisfy Eq. (5), which is the same as Eq. (1). This argument holds when the coupling interaction $\hat{V}$ is not Hermitian and also when it has an energy dependence that is compatible with the conditions for Eq. (4).

For the case of the non-Hermitian Hamiltonian we write

$$\hat{H}_2=\hat{R}+i\hat{I}, \quad \hat{H}_2^-=\hat{R}-i\hat{I} . \tag{10}$$

The polarization potential operator can then be written as

$$\hat{V}_{\mathrm{pol}}(E) =\sum_{r,r'} \hat{V}_{12}|\Phi_{r'}\rangle\left\langle\Phi_{r'}\left|\frac{1}{E-\hat{R}-i\hat{I}+i\epsilon}\right|\Phi_r\right\rangle\langle\Phi_r|\hat{V}_{21} . \tag{11}$$

If one restricts $\hat{I}$ to be diagonal with respect to the states $|\Phi_r\rangle$, this expression reduces to

$$\hat{V}_{\mathrm{pol}}(E)=\sum_r \frac{\hat{V}_{12}|\Phi_r\rangle\langle\Phi_r|\hat{V}_{21}}{E-E_r-iW_r+i\epsilon} , \tag{12}$$

where

$$W_r=\langle\Phi_r|\hat{I}|\Phi_r\rangle \tag{13}$$

is real. Clearly Eq. (12) has the same analytic structure as Eq. (9) when W_r is negative. This case corresponds to typical coupled-channels calculations which use negative imaginary potentials to absorb flux out of excited states. Thus one may expect that such models give results which are consistent with the dispersion relation of Eq. (1).

III. EQUIVALENT LOCAL POTENTIAL

In this section we investigate numerically the so-called trivially equivalent local potential. This provides an intermediate link between the formal operators discussed above and the empirical local potentials obtained from analyzing data.

To define the equivalent local potential, it will suffice to consider a two-channel problem where the intrinsic states have zero spins. The radial wave functions $u_i(r)$ satisfy the coupled equations

$$\left[-\frac{\hbar^2}{2\mu}\frac{d^2}{dr^2}+V_1(r)-E_1\right]u_1(r)=-V_{12}(r)u_2(r) , \tag{14}$$
$$\left[-\frac{\hbar^2}{2\mu}\frac{d^2}{dr^2}+V_2(r)-E_2\right]u_2(r)=-V_{21}(r)u_1(r) .$$

The scattering boundary conditions at large distances require

$$u_i(r)\rightarrow\delta_{i,1}e^{-ik_ir}+r_{i,1}e^{+ik_ir} , \tag{15}$$

where $\hbar^2k_i^2/2\mu=E_i$. Typically one includes absorptive imaginary potentials in $V_i(r)$ and requires regular boundary conditions on the wave functions at the origin. In the calculations presented below flux loss occurs by virtue of in-going wave boundary conditions on the wave functions at short distances.

Having solved the coupled equations under the appropriate boundary conditions, it is a simple matter to obtain the equivalent local potential for the elastic channel as

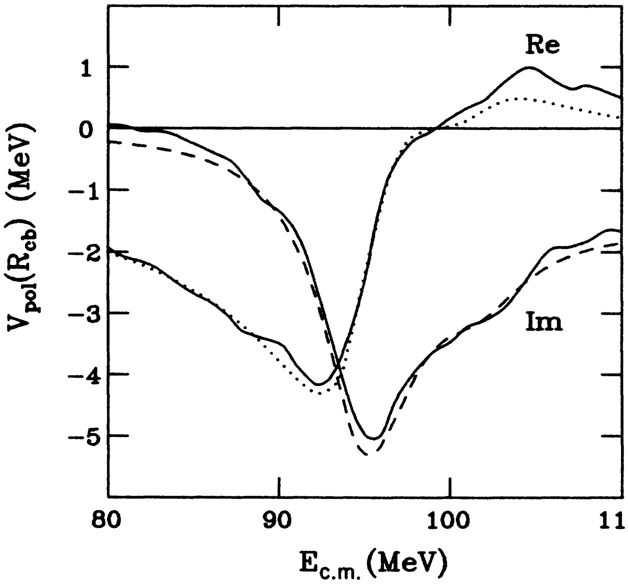

FIG. 1. The equivalent local potential at the Coulomb barrier ($R_{\mathrm{cb}}=10.8$ fm) for ^{58}Ni+^{64}Ni as a function of the center of mass energy (barrier height $V_{\mathrm{cb}}\simeq 98$ MeV). The solid curves are the results of the coupled-channels calculations in Ref. 5. The dashed curve parametrizes the imaginary part with Eq. (18). The dotted curve plots the analytic expression for the real part in Eq. (19) that is predicted by the dispersion relation.

$$V_{\text{pol}}(r)=V_{12}(r)u_2(r)/u_1(r)\ , \tag{16}$$

so that by construction,

$$\left[-\frac{\hbar^2}{2\mu}\frac{d^2}{dr^2}+V_1(r)+V_{\text{pol}}(r)-E\right]u_1(r)=0\ . \tag{17}$$

Thus if one were given the elastic cross section for this problem and asked to determine the effective interaction which produced it, the correct answer would be the sum $V_1(r)+V_{\text{pol}}(r)$, where the second term is distinguished by being energy dependent (it also depends on the total angular momentum). The result of Eq. (16), however, could never be obtained precisely because the elastic cross section at best only determines the reflection coefficients $r_{1,1}$.

A large coupled-channels calculation was carried out in Ref. 5 to simultaneously describe the fusion and direct reactions in $^{58}\text{Ni}+^{64}\text{Ni}$ collisions at energies near the Coulomb barrier. The model used in-going wave boundary conditions to account for the fusion process and contained no additional imaginary potentials. An essential simplification was to employ the rotating frame approximation, which effectively amounts to having a set of states with zero intrinsic spins (for further details, see Ref. 5). The equivalent local potential for the s wave in the elastic channel was presented as a function of energy at a radius corresponding to the barrier position. These results are reproduced by the solid curves in Fig. 1. The barrier height in this case is about 98 MeV.

It was remarked in Ref. 5 that the real and imaginary parts of the equivalent local potential appear to satisfy a dispersion relation. Here we demonstrate that this is true to a good accuracy. We have parameterized the imaginary part of the effective potential as

$$\text{Im}V_{\text{pol}}(E)=\frac{-A}{\alpha^2+(E-E_0)^2}+\frac{-B(E-E_0)^2}{\beta^2+(E-E_0)^2}\bigg|_{E>E_0}+\frac{-C}{\gamma^2+(E-E_1)^2}\ , \tag{18}$$

with $A=47.03$, $B=1.55$, $C=10.353$, $\alpha^2=9.2043$, $\beta^2=5.272$, $\gamma^2=11.9$, $E_0=95.1$, and $E_1=101.7$. The result is shown by the dashed curve in Fig. 1. Using this expression in the subtracted form[1] of Eq. (1) generates the real part as (setting $E_t=-\infty$),

$$\text{Re}V_{\text{pol}}(E)=F(E)-F(\bar{E})\ ,$$

$$F(E)=\frac{A}{\alpha}\frac{E-E_0}{(E-E_0)^2+\alpha^2}+\frac{C}{\gamma}\frac{E-E_1}{(E-E_1)^2+\gamma^2}+\frac{B}{(E-E_0)^2+\beta^2}\left[\frac{(E-E_0)^2\ln|E-E_0|+\beta^2\ln\beta}{\pi}-\frac{\beta(E-E_0)}{2}\right]. \tag{19}$$

This formula with $\bar{E}=99.13$ MeV reproduces the numerical results for the real potential very well, as shown by the dotted curve in Fig. 1.

We have made similar comparisons at other distances, including the position inside the barrier where the in-going wave condition was applied. Here the energy dependence is more complicated than in Fig. 1. This causes the parametrization of the imaginary part to be more ambiguous and the reproduction of the real part to be less precise than the example above. It is our conclusion that the dispersion relation is also reasonably well satisfied at other distances, to within the uncertainties of our parametrizations. Thus the feature that the dispersion relation of Eq. (1) is independent of any spatial properties of the operators also appears to be reflected in the equivalent local potential.

There is another obvious property of the effective potential operator in Eq. (2) that is not apparent in the equivalent local potential of Eq. (16). Equation (2) is independent of the Hamiltonian in the entrance channel, while Eq. (16) depends explicitly on the entrance channel wave function. We have made additional calculations to investigate this point. The same case was used as in Fig. 1 except, for simplicity, only a single inelastic channel was included in the coupled equations.

The solid curves in Fig. 2 show the results for the equivalent local potential at the barrier position for this simplified problem. They are completely analogous to the results in Fig. 1 in that in-going wave boundary conditions have been used in all channels and no absorptive potentials are present. It is again apparent that the dispersion relation is satisfied. The dashed curves in Fig. 2 are obtained after including an absorptive potential of

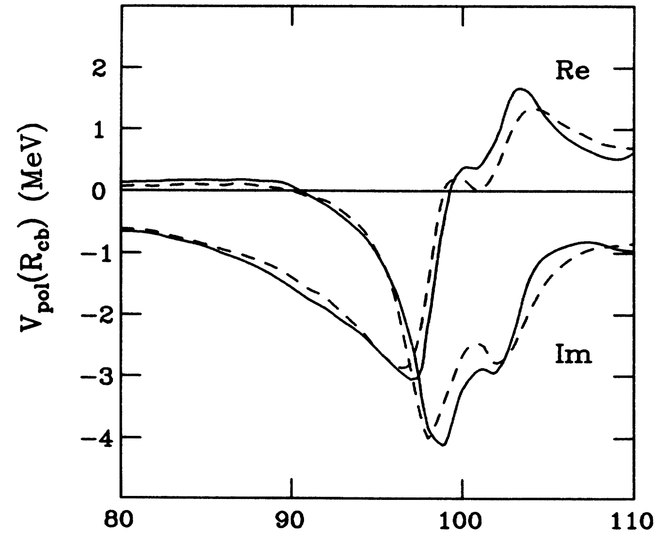

FIG. 2. The equivalent local potential as in Fig. 1 for a simplified case where only one excited state couples to the entrance channel. The solid curves result when in-going wave boundary conditions are made in both channels and no absorptive potentials are present. The dashed curves include a typical absorptive potential in the elastic channel only.

the Woods-Saxon type normally used for optical model calculations ($W=-20$ MeV, $R_w=9.35$ fm, $a_w=0.63$ fm) in the elastic channel only. Although this obviously distorts the elastic wave and changes the reaction cross section, Fig. 2 shows that practically no change occurs in the equivalent local potential.

The solid curves in Fig. 3 are obtained after introducing the absorptive potential in the inelastic channel only. This changes the equivalent local potential from that shown in Fig. 2, but clearly does not alter the dispersion relation between its real and imaginary parts. It is easy to demonstrate this with the fitting procedure described above. In this way we have specifically checked that the non-Hermitian character of the excited state Hamiltonian does not affect the dispersion relation.

Finally, the dashed curves in Fig. 3 complete this set of calculations by including the absorptive potential in both channels. They illustrate once more that the equivalent local potential does not depend strongly on the bare potential used in the elastic channel when solving the coupled equations.

IV. CONCLUSION

In this work we have argued that the dispersion relation for the effective potential operator holds true when the Hamiltonian is not Hermitian, as is the case in practically all nuclear reaction calculations. We have also verified by way of examples that the equivalent local potential has the properties expected for the effective potential operator to within a good approximation. In particular, it exhibits the dispersion relation when absorption is present. We have also verified that the equivalent local potential is insensitive to the potential used in the elastic channel when solving the coupled equations. The fact that the local equivalent potential in realistic model calculations closely follows the dispersion relation adds theoretical support to the energy-dependent local potentials that have been determined empirically.

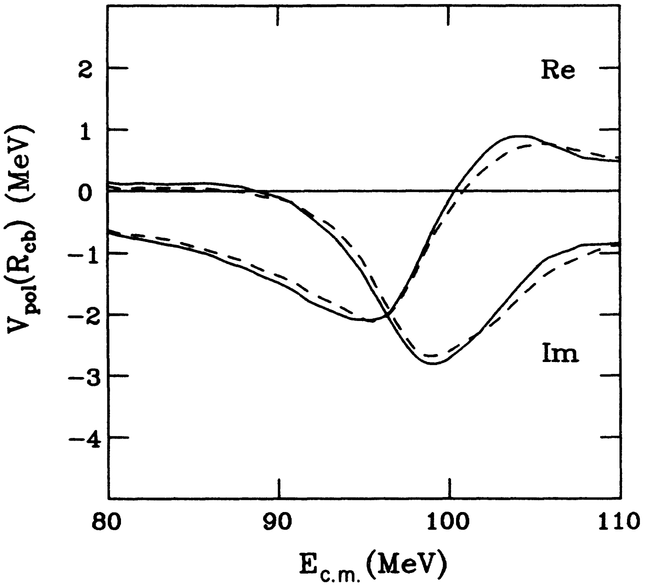

FIG. 3. Calculations similar to those in Fig. 2. The solid curves result when the absorptive potential is added to the inelastic channel only. The dashed curves include absorptive potentials in both channels.

ACKNOWLEDGMENTS

Research at the Centro Técnico Aeroespacial, Instituto de Estudos Avançados was supported in part by the Conselho Nacional de Desenvolvimento Científico e Tecnologico (CNPq). Work at the Argonne National Laboratory was supported by the U.S. Department of Energy, Nuclear Physics Division, under Contract No. W-31-109-Eng-38.

---

[1] M. A. Nagarajan, C. Mahaux, and G. R. Satchler, Phys. Rev. Lett. **54**, 1136 (1985).

[2] C. Mahaux, H. Ngô, and G. R. Satchler, Nucl. Phys. **A449**, 354 (1986).

[3] H. Feshbach, Ann. Phys. (N.Y.) **5**, 357 (1958).

[4] H. W. Wyld, *Mathematical Methods for Physics* (Benjamin/Cummings, Reading, Mass., 1976).

[5] H. Esbensen and S. Landowne, Nucl. Phys. **A492**, 473 (1989).